Article

Superoxide Dismutase Detection on Silver Nanostructured Substrates through Surface-Enhanced Spectroscopic Techniques

Anastasia Kanioura [1,*], Georgia Geka [1], Ioannis Kochylas [2], Vlassis Likodimos [2], Spiros Gardelis [2], Anastasios Dimitriou [3], Nikolaos Papanikolaou [3], Sotirios Kakabakos [1] and Panagiota Petrou [1,*]

[1] Immunoassays/Immunosensors Lab, Institute of Nuclear & Radiological Sciences & Technology, Energy & Safety, NCSR "Demokritos", 15341 Aghia Paraskevi, Greece; g.geka@rrp.demokritos.gr (G.G.); skakab@rrp.demokritos.gr (S.K.)
[2] Section of Condensed Matter Physics, Department of Physics, National and Kapodistrian University of Athens, University Campus, 15784 Athens, Greece; ikochyla@phys.uoa.gr (I.K.); vlikodimos@phys.uoa.gr (V.L.); sgardelis@phys.uoa.gr (S.G.)
[3] Institute of Nanoscience & Nanotechnology, NCSR "Demokritos", 15341 Aghia Paraskevi, Greece; a.dimitriou@inn.demokritos.gr (A.D.); n.papanikolaou@inn.demokritos.gr (N.P.)
*   Correspondence: nkanioura@ipta.demokritos.gr (A.K.); ypetrou@rrp.demokritos.gr (P.P.); Tel.: +30-210-650-3819 (A.K.)

Abstract: Oxidative stress refers to the overproduction of reactive oxygen species and is often associated with numerous pathological conditions. Superoxide dismutase (SOD) is a widely used enzyme for evaluating oxidative stress, with numerous methods being developed for its detection in biological specimens like blood, urine, and saliva. In this study, a simple metal-assisted chemical etching method was employed for the fabrication of nanostructured silicon surfaces decorated with either silver dendrites or silver aggregates. Those surfaces were used as substrates for the immunochemical determination of SOD in synthetic saliva through surface-enhanced Raman spectroscopy (SERS) and surface-enhanced fluorescence (SEF). The immunoassay was based on a 3-step competitive assay format, which included, after the immunoreaction with the specific anti-SOD antibody, a reaction with a biotinylated secondary antibody and streptavidin. Streptavidin labeled with peroxidase was used in combination with a precipitating tetramethylbenzidine substrate for detection through SERS, whereas for SEF measurements, streptavidin labeled with the fluorescent dye Rhodamine Red-X was utilized. Both immunoassays were sensitive, with a detection limit of 0.01 µg/mL and a linear dynamic range from 0.03 to 3.3 µg/mL, enabling the evaluation of the oxidative stress status of an organism.

Keywords: superoxide dismutase; competitive immunoassay; surface-enhanced photoluminescence; surface-enhanced Raman spectroscopy

1. Introduction

Superoxide dismutase (SOD) is an essential enzyme that plays a crucial role in antioxidant defense mechanisms in living organisms. There are three main types of superoxide dismutase found in different cellular compartments: cytoplasmic or Cu/Zn-SOD (SOD1), mitochondrial or Mn-SOD (SOD2), and extracellular or EC-SOD (SOD3) [1]. The primary function of SOD is to catalyze the dismutation of superoxide radicals into oxygen and hydrogen peroxide [2]. Superoxide radicals are highly reactive and may cause cellular damage by initiating oxidative stress. The balance between the production of reactive oxygen species (ROS) and the activity of antioxidant enzymes like superoxide dismutase is crucial for maintaining cellular homeostasis [3]. The importance of superoxide dismutase, however, extends beyond cellular protection, as alterations in SOD levels and activity may contribute to the pathogenesis of several diseases, such as diabetes, amyotrophic lateral sclerosis (ALS), and certain types of cancers [1].

Due to the severe impact of SOD on human health, several methods have been developed mainly for the assessment of SOD activity, while only a few reports have been published for the determination of SOD levels in body fluids, based mainly on enzyme immunoassay methods (ELISAs) [4,5]. Although ELISA is a highly sensitive technique, the fact that is laboratory bound and not appropriate for point-of-care determinations led to the development of spectroscopic methods for SOD detection. These methods rely on either surface-enhanced Raman spectroscopy (SERS) [6–10] or surface-enhanced fluorescence (SEF) [11], employing aptamers [6–8] or antibodies [10,11] as biorecognition molecules for the determination of SOD levels.

Surface-enhanced Raman spectroscopy (SERS) is a powerful analytical technique used for the detection and characterization of molecules, including metabolites, disease biomarkers, food contaminants, environmental hazards, etc., at very low concentrations [12–14]. The technique relies on the Raman scattering phenomenon, in which molecules disperse light at wavelengths distinct from the incident light as a result of resonance with their vibrational modes [15]. The enhancement in Raman scattering is due to the interaction between the molecules being analyzed and the surface plasmons of small metallic structures. This interaction leads to a substantial increase in the strength of the electromagnetic field around the metal surface, up to a factor of 10^{10}, which is particularly pronounced in clusters of metallic particles, known as "hot spots" [16,17]. Surface-enhanced fluorescence (SEF) is a phenomenon closely associated with surface-enhanced Raman spectroscopy (SERS), but it focuses on the amplification of the fluorescence signal of molecules instead of Raman scattering [18]. In this case, the enhancement in fluorescence arises from the interaction between fluorophores and the localized surface plasmons (LSPs) of metallic nanostructures [19]. When fluorophores adhere to or are positioned near these nanostructures, the electromagnetic field amplification caused by localized surface plasmons (LSPs) leads to elevated rates of both excitation and emission, resulting in enhanced fluorescence intensity [19]. The enhancement factors provided by SEF range from 10^2 to 10^6 depending on the specific experimental conditions and fluorophore–nanostructure interactions [20].

The choice and design of the substrate are crucial for maximizing enhancement in both spectroscopic techniques. Several methods such as colloidal synthesis, lithography, self-assembly and etching techniques have been used to fabricate substrates with well-defined nanostructures tailored to specific applications [21–26]. Common morphologies include nanoparticles, nanopillars, nanostars, nanorods, nanowires, and hierarchical structures. Each morphology provides distinctive advantages in terms of reproducibility and sensitivity in the detection of analytes [27–31]. The most widely used substrates in SERS and SEF are based on metals such as silver, gold or copper. Gold nanoparticles are highly stable in various chemical environments and exhibit strong plasmonic properties; however, their fabrication is relatively expensive [32]. Copper offers a cost-effective alternative to gold nanoparticles. Copper nanoparticles also exhibit plasmonic properties, although typically in the near-infrared (NIR) range, which may be a drawback for certain applications. Furthermore, copper is more susceptible to oxidation and surface contamination, which may affect the reproducibility and stability of the measurements [33]. On the other hand, silver nanoparticles exhibit the highest enhancement factors among the three noble metals and are frequently used for the detection of biomolecules, including proteins, nucleic acids, and small molecules, in complex biological samples such as blood, urine, and tissues, despite also being prone to oxidation [34]. The strong localized surface plasmon resonance (LSPR) characteristics of silver nanoparticles are the result of the coordinated oscillation of unbound electrons in reaction to incoming light, and it can be manipulated by changing the dimensions, configuration, and organization of the silver nanostructures [35].

Another important factor in signal enhancement is the selection of the appropriate Raman label and fluorophore in SERS and SEF, respectively. Raman labels are molecules with a strong Raman signal and are frequently used for the detection of molecules with low Raman sensitivity. Moreover, Raman labels should have distinguishable spectral features that allow for the easy identification and quantification of analytes [36]. Commonly

used Raman labels in SERS include organic dyes (e.g., rhodamine 6G, crystal violet), aromatic thiols (e.g., p-mercaptobenzoic acid), and other molecules with strong Raman scattering properties, such as tetramethylbenzidine [37,38]. SEF fluorophores should be also selected on the basis of maximizing signal enhancement and, therefore, detection sensitivity. For optimal signal amplification, a fluorophore should have high quantum yield, a large absorption cross-section, photostability, and chemical stability to prevent signal fluctuations or deterioration during SEF experiments. Additionally, the fluorophores' emission wavelength should match the nanostructures' excitation and plasmon resonance in SEF substrates [20]. Some of the most widely used fluorophores in SEF include fluorescein, ATTO dyes, Alexa Fluor dyes, Quantum dots and Rhodamine derivatives [39].

The aim of this work was to develop a sensitive immunochemical approach for the spectroscopic detection of superoxide dismutase in synthetic saliva, through SEF and SERS, so as to be able to compare the two detection approaches using the same reagents and assay procedure. For this reason, two distinct configurations of silver nanoparticles were fabricated on silicon surfaces with a simple metal-assisted chemical etching process and evaluated as substrates for the detection of SOD. Our team has already successfully employed these substrates for the determination of two oxidative stress markers, namely glutathione and malondialdehyde, and for the ovarian cancer markers Ca125 and HE4, indicating the potential of these metallic nanostructures in the detection of biological molecules at low concentrations [40,41]. The protocol for SOD determination was based on a competitive immunoassay configuration, and two different signal enhancement approaches were investigated. Thus, after the immunoreaction with the primary anti-SOD monoclonal antibody, a reaction with an anti-species specific (secondary) antibody took place. The secondary antibody was used either in unlabeled form or after biotinylation to enable further signal enhancement and the improvement of detection sensitivity through a reaction with streptavidin. The parameters of the SERS and SEF-based immunoassay have been optimized and a comparison of their analytical performance with other literature methods is also provided.

2. Materials and Methods

2.1. Materials

Nitric acid (HNO_3) was obtained from Lach-Ner Ltd. (Neratovice, Czech Republic). Hydrofluoric acid (HF) was obtained from Technic Inc. (Saint-Denis, France). Silver nitrate ($AgNO_3$), superoxide dismutase from human erythrocytes (2500 U/mg), mouse monoclonal antibody against superoxide dismutase (clone SD-G6), streptavidin–peroxidase polymer (streptavidin–HRP), and tetramethylbenzidine precipitating membrane substrate were purchased from Sigma-Aldrich (Darmstadt, Germany). The bovine serum albumin (BSA) was from Acros Organics (Geel, Belgium). Streptavidin conjugated with Rhodamine Red-X and anti-mouse antibody conjugated with Alexa Fluor 546 were obtained from ThermoFischer Scientific (Waltham, MA, USA). Twenty-four-well culture plates were obtained from Greiner Bio-One GmbH (Kremsmünster, Austria). All other chemicals used were of analytical grade and were purchased from Merck (Darmstadt, Germany). The water used was distilled.

2.2. Fabrication and Characterization of Substrates for SEF/SERS

The silver substrates were fabricated with a simple metal-assisted chemical etching (MACE) procedure, as previously described [24,40]. Our study focused on evaluating the performance of two distinct substrate types: one containing Ag dendrite-decorated Si nanowires (SiNWs) (type A) and the other containing Ag aggregate-decorated Si nanowires (type B), both created onto p-type (100) oriented monocrystalline silicon wafers. For the fabrication of type A substrates, the wafers were dipped for 3.5 min into an aqueous solution containing a mixture of $AgNO_3$ and HF with concentrations of 0.02 M and 4.8 M, respectively. For the creation of type B substrates, the silicon wafers were dipped first for 7 min in the $AgNO_3$/HF mixture and then into a 50% *v/v* HNO_3 aqueous solution for

4 min to dissolve the Ag structures formed during the first step. Finally, the wafers were re-immersed into the AgNO$_3$/HF mixture for 7 s, resulting in the formation of aggregated Ag nanoparticles on the SiNWs tips.

The substrates produced employing this process were analyzed at each step using scanning electron microscopy (SEM) with a JSM-7401F SEM apparatus (JEOL Europe bv; Zaventem, Belgium) running at 30 kV.

2.3. Preparation of Synthetic Saliva Samples

A synthetic saliva matrix was prepared based on a published protocol [42] and used for the preparation of the SOD calibrators. In particular, this matrix contained 0.13 g/L NaCl, 0.96 g/L KCl, 0.66 g/L KH$_2$PO$_4$, 0.63 g/L NaHCO$_3$, 0.19 g/L KSCN, 0.23 g/L CaCl$_2$, 0.2 g/L urea, 0.76 g/L Na$_2$SO$_4$, and 0.18 g/L NH$_4$Cl. Before it was used for the preparation of the SOD calibrators, the pH of the synthetic saliva was adjusted to 6.8.

2.4. Detection of SOD with Enzyme-Linked Immunosorbent Assays

For SOD determination a 3-step competitive immunoassay configuration was followed. According to that, 96-well ELISA microtitration plates were incubated with 100 μL per well of a 5.0 μg/mL SOD solution in 50 mM carbonate buffer, pH 9.2, overnight at RT. Afterwards, the wells were washed twice with 300 μL of PBS 10 mM, pH 7.4, and were blocked through incubation for 1 h with 300 μL of a 10 mg/mL BSA solution in 0.1 M NaHCO$_3$, pH 8.5 (blocking solution). SOD calibrators at concentrations ranging from 0.03–3.3 μg/mL, prepared either in assay buffer (PBS 50 mM, 10 mg/mL BSA, pH 7.4) or synthetic saliva, were mixed at a 1:1 volume ratio with a 0.5 μg/mL anti-SOD monoclonal antibody prepared in assay buffer, and incubated for 1 h. Then, the wells were rinsed as before and 100 μL of each calibrator/anti-SOD antibody mixture were added and incubated for 1 h under shaking. Another washing step followed, prior to incubation with 100 μL of a 5.0 μg/mL biotinylated anti-mouse IgG antibody solution in assay buffer for 30 min. Then, the wells were rinsed four times with PBS 10 mM, pH 7.4, containing 0.5 mL/L Tween 20 and 100 μL of a 50 ng/mL streptavidin–HRP solution in 50 mM PBS, pH 6.5, 10 g/L BSA, were added and incubated for 30 min under shaking. Finally, the wells were washed as before, and incubated under shaking with 100 μL of HRP substrate (0.03% *v/v* H$_2$O$_2$ and 1.9 μM ABTS in 0.1 M citrate-phosphate buffer, pH 4.5), prior to the measurement of the wells' optical density at 405 nm using a VICTOR3 1420 Multilabel Counter (PerkinElmer).

2.5. SOD Immunochemical Determination through SEF

Substrates with area of 0.25 cm^2 were placed in 24-well polystyrene plates (Figure S1) and incubated with a 5.0 μg/mL SOD solution in 50 mM carbonate buffer, pH 9.2, overnight at 4 °C. Then, the substrates were washed twice with 300 μL of PBS 10 mM, pH 7.4, and the free binding sites were blocked though incubation with 300 μL of blocking solution for 1 h. SOD calibrators at concentrations ranging from 0.03–3.3 μg/mL, prepared either in assay buffer (PBS 50 mM, pH 7.4, 10 mg/mL BSA) or synthetic saliva, were mixed at a 1:1 volume ratio with a 0.5 μg/mL anti-SOD monoclonal antibody solution prepared in assay buffer and incubated for 1 h. Then, the substrates were rinsed as before and 200 μL of each calibrator/antibody mixture were added into the wells and incubated for 1 h under gentle shaking. After washing the substrates as before, 200 μL of a 5.0 μg/mL biotinylated anti-mouse IgG antibody solution in assay buffer were added per well and incubated for 30 min. Next the substrates were rinsed four times with PBS 10 mM, pH 7.4, containing 0.5 mL/L Tween 20, and 200 μL of a 5.0 μg/mL streptavidin–Rhodamine Red-X solution in 50 mM PBS, pH 6.5, 10 g/L BSA, were added per well and incubated for another 30 min. Before measuring the SEF intensity, the surfaces were rinsed thrice with PBS and once with distilled water. The non-specific binding was determined from substrates non-coated with SOD (blank) which were treated as the substrates corresponding to the zero calibrator. A schematic of SEF assay is provided in Figure 1.
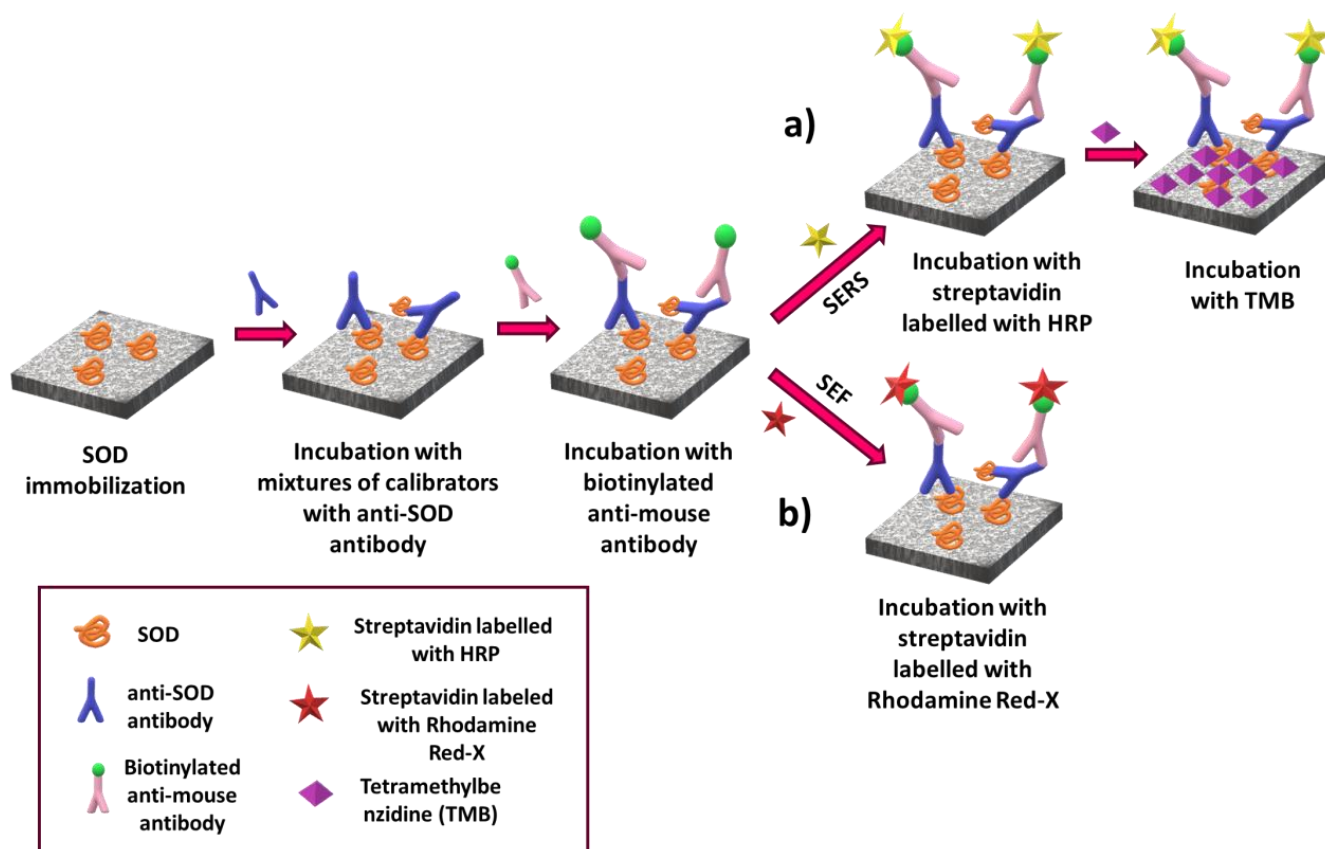
Figure 1. Schematic of the assay steps followed for SOD determination by (**a**) SEF and (**b**) SERS.

The fluorescence signal intensity was measured using a custom-made apparatus comprising a green diode laser (532 nm wavelength) that illuminated the samples at a 45-degree angle via a focusing lens. The laser intensity on the sample was approximately 2 mW, the diameter of the illuminated region was approximately 2 mm, and the exposure time was less than 15 s. Under these exposure conditions, both the sample heating and quenching of the fluorescence signal intensity were minimal. The emitted fluorescence was collected by an optical fiber, through a long-pass filter to minimize interference from the excitation light, and it was driven to a spectrophotometer (Ocean Insight; Duiven, The Netherlands). In all cases three sample replicates were measured and five spectra were collected from each sample. The intensity corresponding to the non-specific binding was subtracted from the mean maximum intensity of the SEF spectra of each calibrator and the net signals were calculated. For the preparation of the calibration curves, the percentage of the net SEF intensity corresponding to the different calibrators, to the net SEF intensity of the zero calibrator, was plotted versus the SOD concentration.

2.6. SOD Immunochemical Determination through SERS

The approach for determining SOD on silver nanostructured surfaces using SERS was the same as that followed for the SEF measurements, up to the point of incubation with the streptavidin solution. In the case of the SERS measurements, the substrates were incubated for 30 min under gentle shaking with 200 μL of a 50 ng/mL streptavidin–HRP solution in 50 mM PBS, pH 6.5, 10 g/L BSA. Then, the surfaces were rinsed three times with PBS 10 mM, pH 7.4, containing 0.5 mL/L Tween 20, and one time with distilled water and incubated with 200 μL of precipitating TMB substrate for 3 min. After, rinsing four times with water, the Raman spectra of the substrates were acquired with an inVia Reflex microscope (Renishaw, UK) equipped with a solid-state laser that emits light at 785 nm. The laser beam was concentrated onto the samples to a spot size of approximately 1 μm

using a 50x (NA = 0.75) objective lens. To prevent local heating effects, the laser's power density was kept at 0.06 mW/μm^2, and the integration time was fixed at 10 s. The net SERS intensity and the calibration curve were calculated as described in the previous section for the SEF measurements. A schematic of SERS assay is provided in Figure 1.

3. Results

The substrates utilized in this work were fabricated with the MACE method, and included SiNWs decorated with either Ag dendrites or Ag nanoparticle aggregates. The substrates with the Ag dendrites were selected for the SEF measurements while those with the Ag aggregates were employed for the SERS measurements, based on previous findings that indicated Ag dendrites were more effective in SEF, whereas aggregates exhibited a higher signal and an enhanced reproducibility in SERS measurements [40,41].

The determination of SOD was based on a competitive immunoassay format, where the signal is inversely proportional to the analyte concentration in the sample, and the detection sensitivity is defined by the percent signal drop of the calibrators containing known amounts of analyte to the signal obtained for the zero calibrator. Two different assay configurations were investigated in order to select the one providing the highest assay sensitivity. The first configuration involved after the primary immunoreaction, i.e., the reaction of the calibrator or sample with the anti-SOD antibody, reaction with an appropriately labelled secondary antibody for the acquisition of SEF or SERS signal, and it would thereby later be referred to as a 2-step assay. The second one, after the primary immunoreaction, involved incubation with a biotinylated secondary antibody followed by a reaction with appropriately labelled streptavidin, and it would later be referred to as a 3-step assay. For both configurations, critical parameters were optimized in terms of SEF and SERS signal intensity and assay sensitivity, such as the concentration of SOD for coating of the substrates, the anti-SOD antibody concentration, and the duration of each assay step.

3.1. Optimization of the 2-Step Assay Configuration

For the detection of SOD following the 2-step assay configuration, the first parameter optimized was the concentration of SOD used for coating of the substrates in combination with different concentrations of the anti-SOD antibody. For this reason, SEF substrates were coated with SOD solutions of different concentrations and then incubated for 1 h with different concentrations of anti-SOD antibody. As shown in Figure 2a, for all anti-SOD antibody concentrations tested, maximum plateau values were obtained when the concentration of SOD solution used for coating of the substrates was equal to or higher than 20 $\mu g/mL$. Regarding the anti-SOD antibody concentration, an increase of the concentration from 2.5 to 5.0 $\mu g/mL$ resulted in a marginal increase (less than 10%) of the signal. Thus, a SOD concentration of 20 $\mu g/mL$ was selected for coating in combination with a 2.5 $\mu g/mL$ anti-SOD antibody concentration.

Using the selected SOD and anti-SOD antibody concentrations, the effect of primary immunoreaction duration on the zero calibrator signal and assay sensitivity was investigated. As indicated in Figure 2b, the SEF signal intensity increase was notable when the incubation time was prolonged to 3 h (28% increase with respect to 2 h), whereas further extension of the primary immunoreaction duration did not provide a further increase of SEF intensity values. Moreover, the assay sensitivity, as indicated from the percent signal values corresponding to the calibrator containing 0.25 $\mu g/mL$ SOD with respect to the zero calibrator, was slightly improved when the primary immunoreaction duration increased from 2 to 3 h. Thus, a 3 h primary immunoreaction duration was adopted in the final protocol. It should be noted that the secondary antibody was used in all cases in excess (10 $\mu g/mL$) and the secondary immunoreaction duration was 1 h.

(**a**)

(**b**)
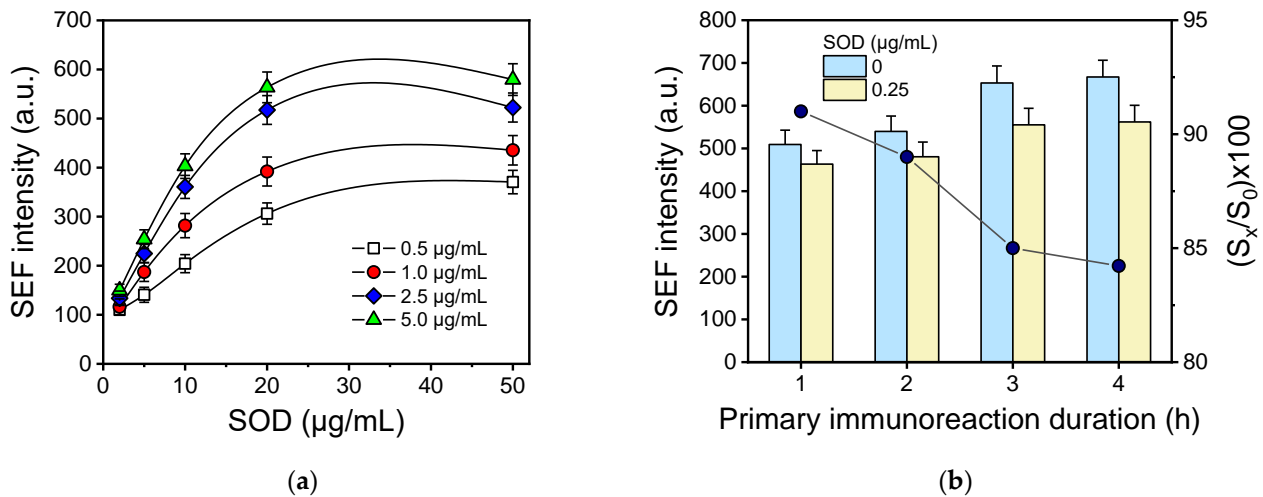
Figure 2. (**a**) Zero calibrator SEF intensity values obtained following the 2-step assay format for different SOD concentrations used for coating in combination with anti-SOD monoclonal antibody concentrations of 0.5 (white squares), 1.0 (red circles), 2.5 (blue diamonds) and 5.0 μg/mL (green triangles). Each point represents the mean value of 5 measurements from 3 different samples ± SD. (**b**) SEF intensity values obtained for the zero calibrator (light blue columns) and a calibrator containing 0.25 μg/mL SOD (light yellow columns) after 1, 2, 3 and 4 h of immunoreaction. Circles correspond to the percent signal drop (right y-axis) obtained for the calibrator containing 0.25 μg/mL SOD with respect to that of the zero calibrator. Each column represents the mean value of 5 measurements from 3 different samples ± SD.

In Figure 3, the SEF calibration curve obtained with the 2-step assay is presented. The non-linear calibration curve is provided in Figure S2. The zero calibrator absolute value ± the standard deviation (SD) of 10 measurements was 655 ± 37 a.u. The limit of detection (LOD) and the limit of quantification (LOQ) were calculated as the SOD concentration that corresponds to the value equal to the zero calibrator value minus 3 and 6 times, respectively, the SD value of 10 repetitive measurements of the zero calibrator. The LOD was 0.16 μg/mL and the LOQ 0.33 μg/mL, and the linear dynamic range of the assay extended to 10 μg/mL.
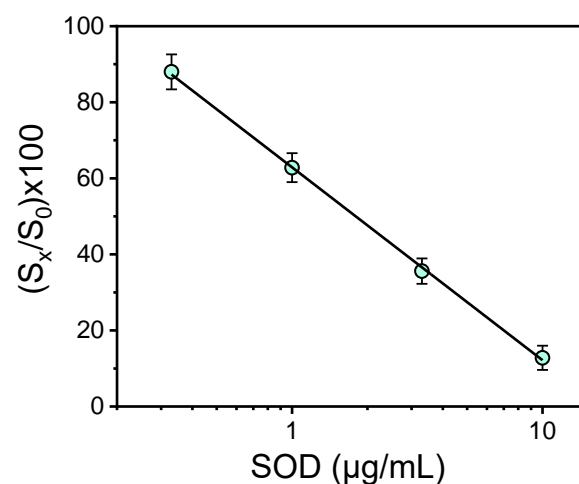
Figure 3. SOD calibration curve in assay buffer obtained employing the 2-step assay configuration. The linear regression equation of the calibration curve is $\log Y = 62.9(\pm 0.6) - 50.7(\pm 0.9)\log X$, and the coefficient of correlation is $R^2 = 0.9993$. Each point represents the mean value of 5 measurements from 3 different samples ± SD.

3.2. Optimization of the 3-Step Assay Configuration

In the 3-step assay configuration, the secondary antibody was biotinylated, and a streptavidin conjugated with the fluorescent dye Rhodamine Red-X was used for SEF measurements. As in the previous configuration, the parameters first optimized were the SOD concentration utilized for the coating of the substrates along with the concentration of anti-SOD antibody. As shown in Figure 4a, the SEF intensity reached maximum plateau values for SOD concentrations in the coating solution equal to or higher than 20 μg/mL. These maximum plateau signal values were approximately 10 times higher than those obtained following the 2-step assay. Moreover, regarding the anti-SOD antibody concentration, the maximum plateau signal values were reached for anti-SOD concentration equal to or higher than 0.5 g/mL. This allowed us to implement much lower concentrations of both SOD for coating and anti-SOD antibody in the primary immunoreaction. Thus, SOD concentrations 5.0 and 10 μg/mL for coating the substrates along with a 0.5 μg/mL antibody concentration were further evaluated in terms of assay sensitivity. As shown in Figure S3, the higher percent signal drop for two SOD calibrators (0.1 and 1.0 μg/mL), with respect to the zero calibrator, were received using a SOD concentration for coating equal to 5.0 μg/mL and, therefore, this concentration was selected for further experimentation.

(**a**)

(**b**)
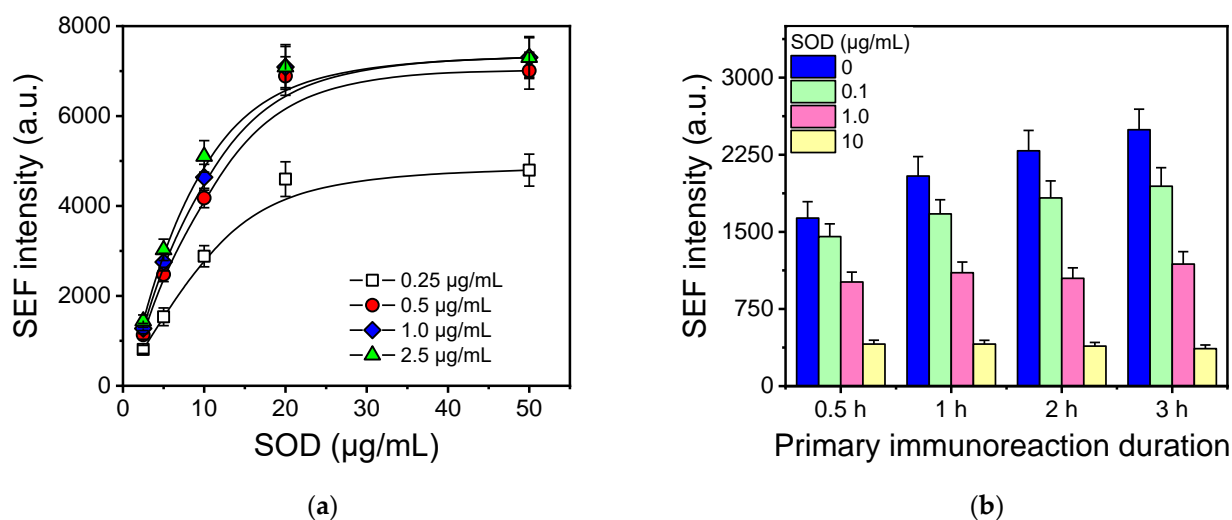
Figure 4. (**a**) Zero calibrator SEF intensity values obtained for different SOD concentrations used for coating the substrates in combination with anti-SOD monoclonal antibody concentrations of 0.25 (white squares), 0.5 (red circles), 1.0 (blue diamonds), and 2.5 μg/mL (green triangles). Each point represents the mean value of 5 measurements from 3 different samples $\pm$ SD. (**b**) SEF intensity values obtained for the zero calibrator (blue columns) and calibrators containing SOD at concentrations 0.1 (green columns), 1.0 (pink columns) and 10 μg/mL (yellow columns) for a primary immunoreaction duration of 0.5, 1, 2 or 3 h. Each column represents the mean value of 5 measurements from 3 different samples $\pm$ SD.

Using the selected SOD concentration for coating and the anti-SOD antibody concentration, the primary immunoreaction duration was re-examined. Thus, mixtures of equal volumes of the anti-SOD antibody solution with SOD calibrators were incubated onto the surfaces for 0.5 to 3 h. The primary immunoreaction was followed by a reaction with a biotinylated secondary antibody and streptavidin labelled with Rhodamine Red-X, both at concentrations of 5.0 μg/mL for 0.5 h. As presented in Figure 4b, when the primary immunoassay duration increased from 0.5 to 1 h, the zero calibrator SEF signal intensity was enhanced by approximately 25%, and the assay sensitivity was also improved. A further extension of the primary immunoreaction to 3 h resulted in a moderate increase of the absolute signal (approximately 20%) and no further improvement in detection sensitivity, and as such 1 h was selected in the final protocol for the primary immunoreaction. Regard-

ing the biotinylated secondary antibody, it was found that maximum plateau values were obtained using concentrations equal to or higher than 10 µg/mL and a reaction duration equal to 1 h (Figure S4). However, more than 75% of the maximum plateau signal could be received using a 5.0 µg/mL secondary antibody concentration for 0.5 h. Thus, these conditions were adopted in the final protocol. For streptavidin labelled with Rhodamine Red-X, the maximum plateau values were obtained for a concentration 5.0 µg/mL and a reaction time of 0.5 h (Figure S5), and were, therefore, used in the final protocol.

The effect of pre-incubation in detection sensitivity was also investigated. For this purpose, the SOD calibrators were mixed at a 1:1 volume ratio with the anti-SOD monoclonal antibody solution and were either applied directly onto the SOD-coated substrates or incubated at RT for different time intervals prior to their reaction with SOD on the substrates. As indicated in Figure 5a, the 15 and 30 min pre-incubation times had no significant effect on the detection sensitivity. However, after a 60 min pre-incubation, the percentage of signal drop for the calibrators containing 0.1 µg/mL and 1 µg/mL SOD, with respect to the zero calibrator, decreased from 82% to 69% and from 54% to 36%, respectively. An extension of pre-incubation time to 90 min did not further improve the detection sensitivity. Thus, a 60 min pre-incubation step was applied to the final protocol and the characteristic calibration curves obtained without and with a 60 min pre-incubation are presented in Figure 5b. Moreover, the comparison of the SOD calibration curves, presented in Figures 3 and 5b, reveal an improvement in the assay sensitivity (lowest detectable concentration) by a factor of 10 when the 3-step assay configuration was applied instead of the 2-step one. This result is mainly due to the implementation of lower SOD concentrations for the coating of the substrates, and the anti-SOD antibody concentration in the primary immunoreaction, which are the two factors determining a competitive assay sensitivity.

(**a**)　　　　　　　　　　　　　　　　(**b**)
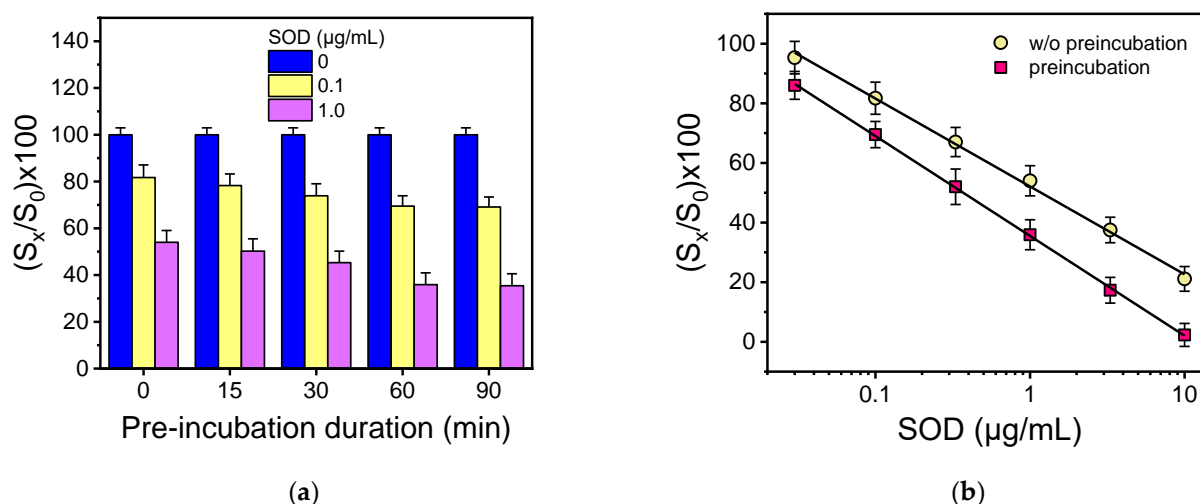
Figure 5. (**a**) Percent signal values obtained for SOD calibrators with concentrations of 0.1 (yellow columns) and 1.0 µg/mL (violet columns) with respect to the zero calibrator values (blue columns) without pre-incubation or after pre-incubation for 15, 30, 60 or 90 min. (**b**) SOD calibration curves obtained without pre-incubation (yellow circles) and after 60 min pre-incubation of the calibrators with the anti-SOD antibody (magenta squares). All values represent the mean of 5 measurements from 3 different samples $\pm$ SD. The linear regression equations of the two curves and the respective coefficients of correlation are as follows: (i) without preincubation: $\log Y = 52.1(\pm0.6) - 29.5(\pm0.7)\log X$; $R^2 = 0.997$, (ii) with preincubation: $\log Y = 35.5(\pm0.3) - 33.5(\pm0.3)\log X$; $R^2 = 0.9997$.

3.3. SOD Determination in Synthetic Saliva through SEF

The effect of synthetic saliva on the assay sensitivity and absolute signal was investigated. In Figure 6, characteristic SEF spectra corresponding to SOD calibrators prepared in assay buffer and synthetic saliva, respectively, are presented. As shown, the presence of synthetic saliva caused an increase in absolute SEF intensity values of about 25%. However,

the respective calibration curves were superimposed, as illustrated in Figure 6c and in the respective non-linear calibration curves presented in Figure S6, demonstrating negligible effect of the calibrators matrix on assay sensitivity.
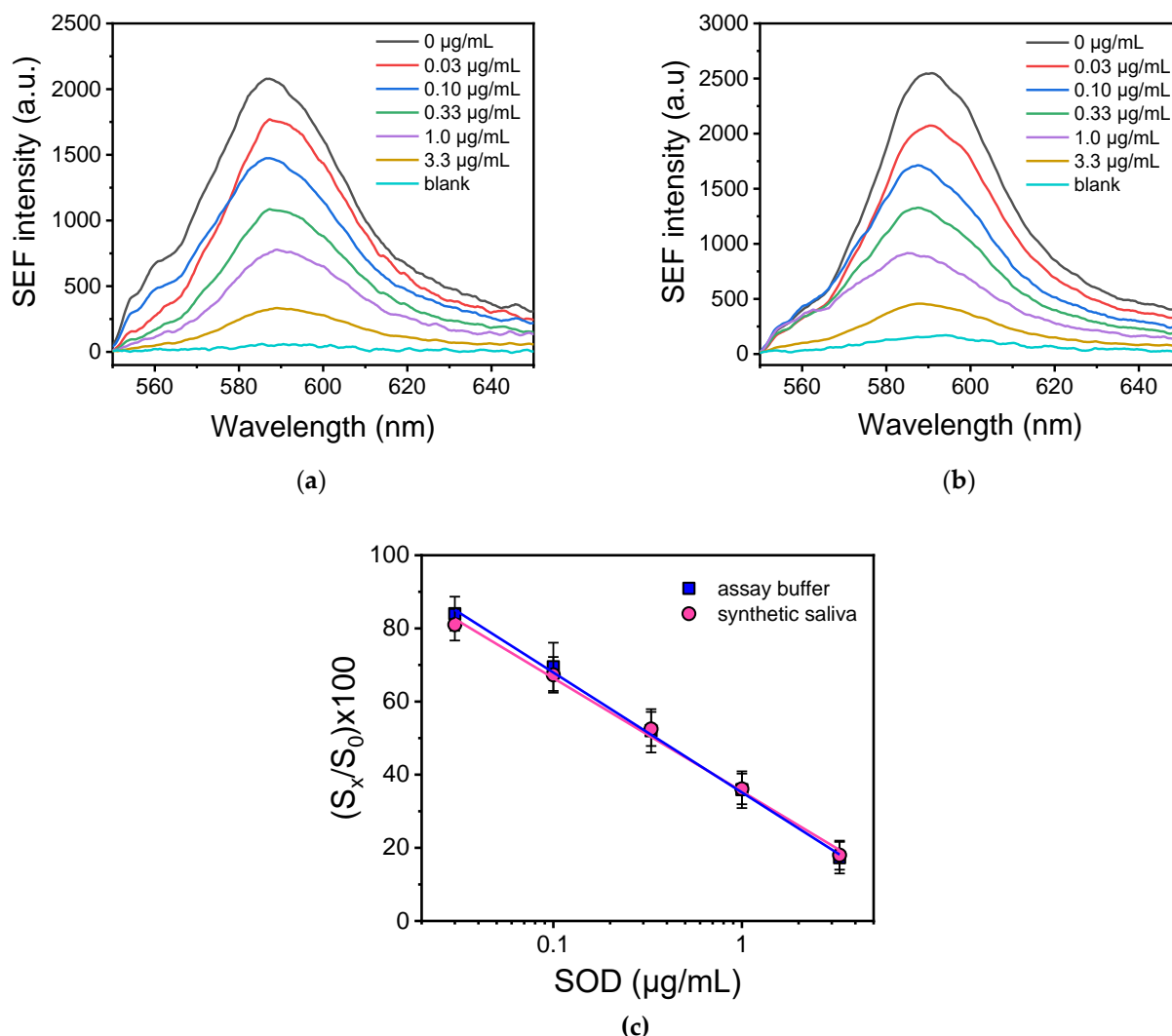
Figure 6. Characteristic SEF spectra obtained for SOD calibrators prepared in (**a**) assay buffer or (**b**) synthetic saliva. (**c**) Characteristic SOD calibration curves obtained with calibrators prepared either in assay buffer (blue squares) or synthetic saliva (pink circles). Each point corresponds to the mean value of 5 measurements from 3 different samples $\pm$ SD. The linear regression equations of the two curves and the respective coefficients of correlation are as follows: (i) assay buffer: $\log Y = 35.4(\pm 0.7) - 32.8(\pm 0.8)\log X$; $R^2 = 0.998$, (ii) saliva: $\log Y = 35.6(\pm 0.9) - 30.9(\pm 1.1)\log X$; $R^2 = 0.996$.

The zero calibrator absolute net value $\pm$ the standard deviation (SD) of 10 measurements were 2024 $\pm$ 58 a.u. in assay buffer and 2547 $\pm$ 78 a.u. in synthetic saliva, respectively. The LOD and LOQ values were determined as described in Section 3.2. The LOD was 0.01 µg/mL and the LOQ was 0.03 µg/mL, and the dynamic range extended from 0.03 to 3.3 µg/mL. The LOD of 0.01 µg/mL corresponds to 0.025 U/mL, and the dynamic range to concentrations from 0.075–0.825 U/mL, as the initial lyophilized reagent contained 2500 U/mg protein, indicating that the method developed was very sensitive and appropriate to determine oxidative stress status in a living organism, as the values in healthy individuals vary from 0.048 to 0.094 U/mL [43,44].

Intra-assay coefficients of variation (CVs), indicative of the within-day variability, were determined through four repetitive measurements of three SOD solutions in synthetic saliva corresponding to different concentration levels (0.05, 0.2 and 2 µg/mL) within a single day, and found to range from 7.3% to 9.1%. Moreover, inter-assay CVs, characterizing the between-day variability, were determined by triplicate measurements of the same SOD solutions at four distinct days over a period of one month and were found to range from 8.4% to 12.2%.

3.4. SOD Determination in Synthetic Saliva through SERS

For SOD determination through SERS, the assay conditions related to the coating of the substrates with SOD, as well as the anti-SOD and secondary antibody concentration and the duration of primary and secondary immunoreaction, were the same as those used in the protocol for SEF measurements. However, since a streptavidin–HRP conjugate was employed for the detection in combination with a precipitating substrate (TMB), the streptavidin–HRP concentration and incubation time with the TMB substrate were optimized. At first, the streptavidin–HRP concentration that provided maximum plateau zero calibrator values was determined at 50 ng/mL for an incubation time of 30 min followed with a reaction of the TMB substrate solution for 10 min. Then, the SERS signals obtained for the zero calibrator and calibrators containing 0.1 and 1 µg/mL SOD were determined for different incubation times with the TMB substrate after a reaction with a 50 ng/mL streptavidin–HRP conjugate for 30 min. As shown in Figure 7, when TMB was added onto the surfaces for 3 min, the intensity values of the calibrators were inversely proportional to their concentration, as is expected for a non-competitive immunoassay. On the other hand, when the TMB was incubated for 10 min, the drop in the SERS intensity values corresponding to the calibrators containing 0.1 and 1 µg/mL SOD with respect to the zero calibrator was negligible. Moreover, when the incubation time with TMB was further increased to 30 min, the SERS intensity obtained for the zero calibrator was lower compared to those received for the calibrators containing SOD. This result is unexpected in a competitive immunoassay; one possible explanation is that the prolonged incubation with the TMB solution resulted in coverage of the surfaces' hot spots by the insoluble TMB product of the enzymatic reaction, thus diminishing the SERS effect. To avoid such phenomena, a 3 min incubation with the substrate was adopted in the final protocol.
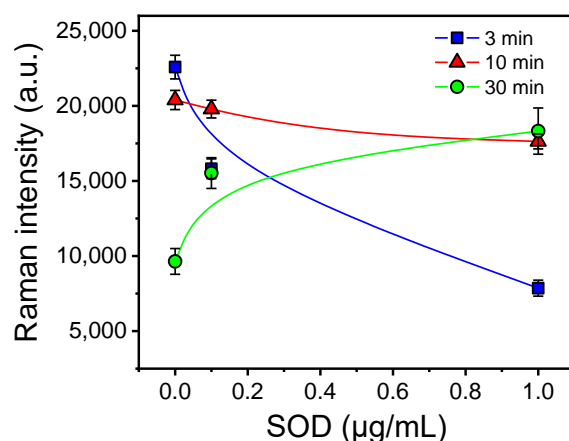
Figure 7. Raman intensity values corresponding to the peak at 1605 cm^{-1} obtained for the zero calibrator and calibrators containing 0.1 and 1.0 µg/mL SOD upon incubation with the TMB precipitating HRP substrate for 3 (blue squares), 10 (red triangles) or 30 (green circles) min. Each point corresponds to the mean value of 5 measurements from 3 different samples ± SD.

In Figure 8, the SERS spectra received for SOD calibrators prepared either in assay buffer (Figure 8a) or synthetic saliva (Figure 8b) are depicted. The respective non-linear calibration curves are provided in Figure S7. As shown, the intensity corresponding to

Raman spectrum peaks of TMB at 1190, 1330, 1400, 1513 and 1605 cm^{-1} were inversely proportional to the SOD concentration, however, the intensity of the peak at 1605 cm^{-1} displayed a bigger percentage change in comparison to the changes noted for the other peaks as the SOD concentration increased and was, therefore, selected as the SERS signal used to fabricate the respective calibration curves. It is worth noting that the presence of synthetic saliva caused an increase in the Raman intensity of all peaks by 15–20%, i.e., the effect was similar to that observed for SEF measurements. As shown in Figure 8c, the calibration curves obtained with calibrators prepared in assay buffer and synthetic saliva were almost identical. The zero calibrator absolute net value $\pm$ the standard deviation (SD) of 10 measurements were 24,655 $\pm$ 518 a.u. in assay buffer and 29,099 $\pm$ 771 a.u. in synthetic saliva, respectively. The analytical characteristics of the SOD SERS assay were calculated as described in Section 3.2. The LOD and the LOQ were 0.015 μg/mL and 0.03 μg/mL, respectively, in both matrices, while the dynamic range extended up to 3.3 μg/mL. In addition, the SERS SOD assay exhibited good repeatability, with inter- and intra-CVs ranging from 7.5 to 10.5%, and from 9.7 to 12.6%, respectively. In other words, the analytical characteristics of the SERS SOD assay were similar to those of the SEF assay. Moreover, the calibration curves obtained using the nanostructured Ag/SiNWs substrates, for either SEF or SERS measurements, were identical to the one obtained by an enzyme immunoassay developed in microtiter plates using the same reagents (Figure S8).

(a)

(b)

(c)
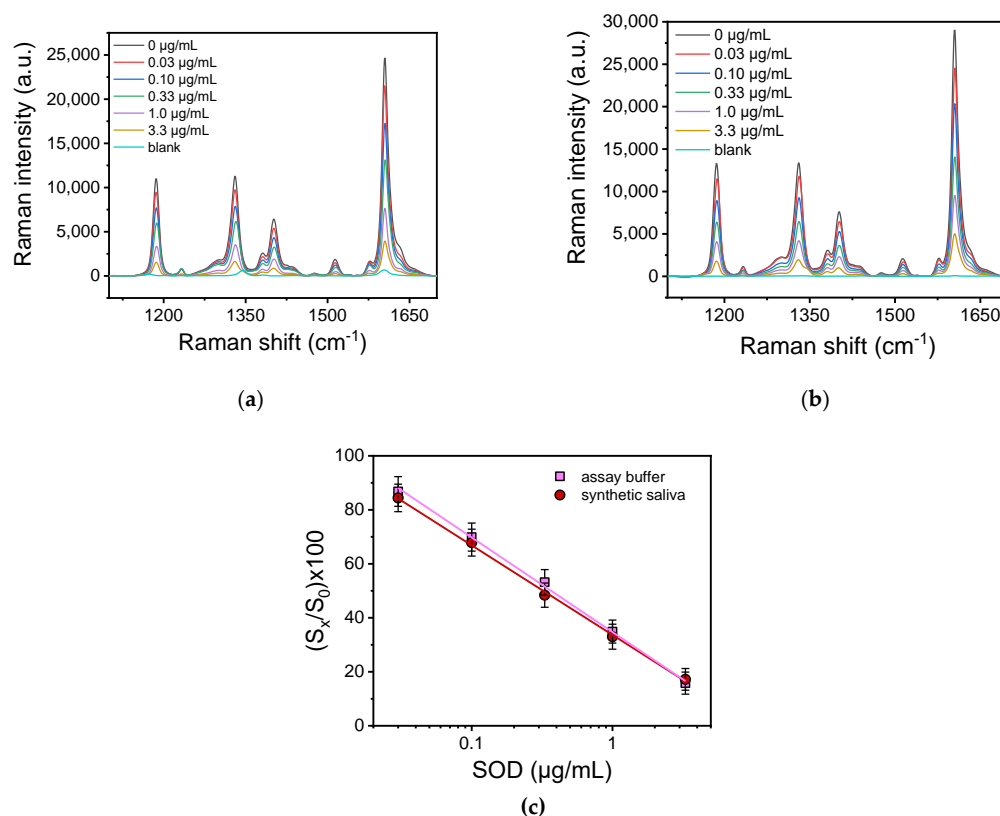
Figure 8. Characteristic SERS spectra obtained for SOD calibrators prepared in (**a**) assay buffer or (**b**) synthetic saliva. (**c**) Characteristic SOD calibration curves obtained with calibrators prepared either in assay buffer (pink squares) or synthetic saliva (wine circles). Each point corresponds to the mean value of 5 measurements from 3 different samples $\pm$ SD. The linear regression equations of the two curves and the respective coefficients of correlation are as follows: (i) assay buffer: $\log Y = 34.8(\pm 0.7) - 34.8(\pm 0.8)\log X$; $R^2 = 0.998$, (ii) saliva: $\log Y = 33.6(\pm 0.6) - 33.3(\pm 0.7)\log X$; $R^2 = 0.998$.

The SEF and SERS assays accuracy was assessed through recovery experiments involving a mixture of saliva samples from five healthy volunteers spiked with three different con-

centrations of SOD (0.07, 0.1, 0.15 and 0.20 µg/mL). Each sample was analyzed three times both before and after spiking with SOD. Recovery values, expressed as percentages of the determined concentration to the added one, were calculated and presented in Table S1. As shown, the recovery values varied from 85.7% to 110%, for both SEF and SERS assay, demonstrating the high accuracy of the methods developed for SOD determination.

3.5. Comparison with Other Spectroscopic Detection Methods

Although the capability to directly detect superoxide dismutase using Raman spectroscopy was demonstrated over a decade ago [45], there are a limited number of publications regarding its quantitative direct determination on SERS substrates. Instead, indirect methods were developed to detect SOD. The type of substrate and label used, as well as the detection limit, dynamic range and duration of the SOD assays reported in the literature are summarized in Table 1 One of these reports presents the detection of SOD on an Au–Ag nanoboxes array modified with the Raman label 4-aminothiophenol (4-ATP). In the presence of SOD, the oxidation of 4-ATP to dithiol azobenzene (DMAB) upon irradiation of the surface at 785 nm in basic conditions (pH 9) was inhibited, enabling the detection of SOD at concentrations of 10–160 U/mL in 20 min [9]. Since the conversion of U to ng of SOD is not provided in this report, to facilitate comparison with the method developed, the limit of detection and dynamic range for our method is provided in Table 1.

Table 1. Comparison of SOD detection with spectroscopic methods.

Substrate	Label	Sample	LOD	Dynamic Range	Analysis Time	Ref
Au–Ag nanoboxes	4-ATP	Blood serum	-	10–160 U/mL	20 min	[9]
Au nanocylinders and nanorods/aptamers	-	Blood serum/saliva	32.5 µg/mL	-	-	[6]
Au nanocylinders/aptamers	-	Assay buffer	3.25 ng/mL	-	-	[7]
Au nanostars/antibody	Au nanostars/ DTNB	Blood serum	0.564 fg/mL	0.1 pg/mL–1000 ng/mL	240 min	[10]
AgNPs/antibody	fluorescein/antibody/ magnetic beads	Assay buffer Blood serum Urine samples Cosmetic samples	4 pg/mL	10 pg/mL–800 ng/mL	60 min	[11]
SiNWs/Ag aggregates	-	Artificial saliva	10 ng/mL 0.025 U/mL	30–330 ng/mL (0.075–0.825 U/mL)	130 min	

There are also two reports for SOD determination using aptamers [6,7]. Both reports employed substrates consisting of gold nano-cylinders or nano-rods created by electron beam lithography and functionalized with thiol-terminated aptamers specific for SOD binding. SOD was determined on both types of substrates at concentrations as low as 100 nM (32.5 µg/mL) in serum and saliva samples [6]. However, a full analytical evaluation of the method is missing. In the second report, principal component analysis was involved to analyze the Raman spectra, and the detection of SOD in concentrations as low as 10 pM (3.25 ng/mL) in assay buffer has been reported, although the main purpose of the study was to define the way SOD interacted with the aptamer [7].

SERS was also employed for the immunochemical detection of misfolded SOD1 in blood serum using a specific monoclonal antibody immobilized on a substrate functionalized with star-shaped gold nanoparticles [10]. The same antibody was conjugated to gold nanoparticles modified with the Raman label 5,5′-dithiobis-(2-nitrobenzoic acid) (DTNB) for the development of a non-competitive immunoassay. A detection limit of 0.564 fg/mL was reported with a very wide dynamic range reaching 1 µg/mL [10].

Regarding the determination of SOD through SEF, there is only one report of a non-competitive immunoassay, where magnetic beads were conjugated with a monoclonal anti-SOD antibody in order to capture the analyte and silver nanoparticles modified with both the anti-SOD antibody and fluorescein-labelled oligonucleotides. A magnetic field

was used to facilitate the separation of bound from free reagents after the completion of the assay. The detection limit was determined at 4 pg/mL and the dynamic range extended up to 800 ng/mL. The method was applied for SOD determination in blood serum, urine and cosmetic samples and the results were in good agreement with those received from a HPLC method [11].

The method developed in this work exhibits similar detection limits with those achieved employing aptamers, but lower detection limits compared to the immunochemical methods reported in the literature. Nonetheless, the LOD and the dynamic range achieved are suitable for SOD determination in saliva [43,44]. In addition, compared to the other approaches reported, the substrates used in the current study are prepared through a simple and comparatively inexpensive method, especially compared to those involving e-beam lithography for the preparation of substrates. It should be noted that the fact that the SEF- and SERS-based immunoassay had the same detection limit, and the dynamic range is to a great extent the result of employing a competitive immunoassay format where the sensitivity is mainly defined by the affinity constant of the antibody used.

4. Conclusions

In this work, two different types of silver nanostructured surfaces were explored as substrates for the immunochemical determination of the oxidative stress marker superoxide dismutase in synthetic saliva through SEF and SERS measurements, respectively. By employing a 3-step assay involving first the primary immunoreaction, then a reaction with a biotinylated antibody and finally with appropriately labeled streptavidin, the detection limit was improved by approximately 10 times and the assay duration was also significantly reduced (from 4 to 2 h) compared to a 2-step assay employing a non-labelled secondary antibody. The detection limit achieved following the optimized assay protocol was 0.01 μg/mL and the dynamic range was extended from 0.03 to 3.3 μg/mL for both SEF and SERS measurements, which are appropriate for the detection of SOD in saliva. In addition, it was observed that the presence of synthetic saliva had a beneficial effect in both SEF and SERS as compared to measurements performed in assay buffer.

References

1. Zeng, M.; Liu, Y.; Zhang, G.; Yang, Z.; Xu, W.; Chen, Q. The Applications and Mechanisms of Superoxide Dismutase in Medicine, Food, and Cosmetics. *Antioxidants* **2023**, *12*, 1675. [CrossRef]
2. MacMillan-Crow, L.A.; Cruthirds, D.L. Invited review: Manganese superoxide dismutase in disease. *Free Radic. Res.* **2001**, *34*, 325–336. [CrossRef]
3. Taverne, Y.J.H.J.; Bogers, A.J.J.C.; Duncker, D.J.; Merkus, D. Reactive Oxygen Species and the Cardiovascular System. *Oxid. Med. Cell. Longev.* **2013**, *2013*, 862423. [CrossRef]
4. Kawaguchi, T.; Suzuki, K.; Matsuda, Y.; Nishiura, T.; Uda, T.; Ono, M.; Sekiya, C.; Ishikawa, M.; Iino, S.; Endo, Y.; et al. Serum-manganese-superoxide dismutase: Normal values and increased levels in patients with acute myocardial infarction and several malignant diseases determined by an enzyme-linked immunosorbent assay using a monoclonal antibody. *J. Immunol. Methods* **1990**, *127*, 249–254. [CrossRef]
5. Ishikawa, M.; Yaginuma, Y.; Hayashi, H.; Shimizu, T.; Endo, Y.; Taniguchi, N. Reactivity of a monoclonal antibody to manganese superoxide dismutase with human ovarian carcinoma. *Cancer Res.* **1990**, *50*, 2538–2542. [CrossRef]
6. Cottat, M.; D'Andrea, C.; Yasukuni, R.; Malashikhina, N.; Grinyte, R.; Lidgi-Guigui, N.; Fazio, B.; Sutton, A.; Oudar, O.; Charnaux, N.; et al. High Sensitivity, High Selectivity SERS Detection of MnSOD Using Optical Nanoantennas Functionalized with Aptamers. *J. Phys. Chem. C* **2015**, *119*, 15532–15540. [CrossRef]
7. Yasukuni, R.; Gillibert, R.; Triba, M.N.; Grinyte, R.; Pavlov, V.; Lamy de la Chapelle, M. Quantitative analysis of SERS spectra of MnSOD over fluctuated aptamer signals using multivariate statistics. *Nanophotonics* **2019**, *8*, 1477–1483. [CrossRef]
8. Dekhili, R.; Cherni, K.; Liu, H.; Li, X.; Djaker, N.; Spadavecchia, J. Aptamer–Gold(III) Complex Nanoparticles: A New Way to Detect Cu, Zn SOD Glycoprotein. *ACS Omega* **2020**, *5*, 13851–13859. [CrossRef]
9. Xia, J.; Chen, G.Y.; Li, Y.Y.; Chen, L.; Lu, D. Rapid and sensitive detection of superoxide dismutase in serum of the cervical cancer by 4-aminothiophenolfunctionalized bimetallic Au-Ag nanoboxs array. *Front. Bioeng. Biotechnol.* **2023**, *11*, 1111866. [CrossRef]
10. Gao, F.; Sun, J.; Yao, M.; Song, Y.; Yi, H.; Yang, M.; Ni, Q.; Kong, J.; Yuan, H.; Sun, B.; et al. SERS "hot spot" enhance-array assay for misfolded SOD1 correlated with white matter lesions and aging. *Anal. Chim. Acta* **2023**, *1238*, 340163. [CrossRef]
11. Yang, X.; Dou, Y.; Zhou, S. Highly sensitive detection of superoxide dismutase based on an immunoassay with surface-enhanced fluorescence. *Analyst* **2013**, *138*, 3246–3252. [CrossRef]
12. Blackie, E.J.; Le Ru, E.C.; Etchegoin, P.G. Single-Molecule Surface-Enhanced Raman Spectroscopy of Nonresonant Molecules. *J. Am. Chem. Soc.* **2009**, *131*, 14466–14472. [CrossRef]
13. Lu, Y.; Lin, L.; Ye, J. Human metabolite detection by surface-enhanced Raman spectroscopy. *Mater. Today Bio* **2022**, *13*, 100205. [CrossRef]
14. Michałowska, A.; Kudelski, A. Plasmonic substrates for biochemical applications of surface-enhanced Raman spectroscopy. *Spectrochim. Acta A Mol. Biomol. Spectrosc.* **2024**, *308*, 123786. [CrossRef]
15. Long, D. 80th anniversary of the discovery of the Raman effect: A celebration. *J. Raman Spectrosc.* **2008**, *39*, 316–321. [CrossRef]
16. Zong, C.; Xu, M.; Xu, L.J.; Wei, T.; Ma, X.; Zheng, X.S.; Hu, R.; Ren, B. Surface-enhanced Raman spectroscopy for bioanalysis: Reliability and challenges. *Chem. Rev.* **2018**, *118*, 4946–4980. [CrossRef]

17. Vo-Dinh, T.; Liu, Y.; Fales, A.M.; Ngo, H.; Wang, H.N.; Register, J.K.; Yuan, H.; Norton, S.J.; Griffin, G.D. SERS nanosensors and nanoreporters: Golden opportunities in biomedical applications. *Nanomed. Nanobiotechnol.* **2015**, *7*, 17–33. [CrossRef]

18. Lakowicz, J.R. Radiative decay engineering 5: Metal-enhanced fluorescence and plasmon emission. *Anal. Biochem.* **2005**, *337*, 171–194. [CrossRef]

19. Parfenov, A.; Gryczynski, I.; Malicka, J.; Geddes, C.D.; Lakowicz, J.R. Enhanced fluorescence from fluorophores on fractal silver surfaces. *J. Phys. Chem. B* **2003**, *107*, 8829–8833. [CrossRef]

20. Lackowicz, J.R.; Geddes, C.D.; Gryczynski, I.; Malicka, J.; Gryczynski, Z.; Aslan, K.; Lukomska, J.; Matveeva, E.; Zhang, J.; Badugu, R.; et al. Advances in Surface-Enhanced Fluorescence. *J. Fluoresc.* **2004**, *14*, 425–441. [CrossRef]

21. Sai, C.D.; Nguyen, Q.H.; Tran, T.N.A.; Pham, V.; Nguyen, T.B.; Do, H.H.; Vu, T.D. CuO nanorods decorated gold nanostructures as an ultra-sensitive and recyclable SERS substrate. *Mater. Chem. Phys.* **2022**, *293*, 126962. [CrossRef]

22. Guselnikova, O.; Lim, H.; Kim, H.J.; Kim, S.H.; Gorbunova, A.; Eguchi, M.; Postnikov, P.; Nakanishi, T.; Asahi, T.; Na, J.; et al. New Trends in Nanoarchitectured SERS Substrates: Nanospaces, 2D Materials, and Organic Heterostructures. *Small* **2022**, *18*, 2107182. [CrossRef] [PubMed]

23. Ma, Y.; Huang, Z.; Li, S.; Zhao, C. Surface-Enhanced Raman Spectroscopy on Self-Assembled Au Nanoparticles Arrays for Pesticides Residues Multiplex Detection under Complex Environment. *Nanomaterials* **2019**, *9*, 426. [CrossRef] [PubMed]

24. Kochylas, I.; Dimitriou, A.; Apostolaki, M.A.; Skoulikidou, M.C.; Likodimos, V.; Gardelis, S.; Papanikolaou, N. Enhanced Photoluminescence of R6G Dyes from Metal Decorated Silicon Nanowires Fabricated through Metal Assisted Chemical Etching. *Materials* **2023**, *16*, 1386. [CrossRef]

25. Bai, S.; Li, Z.X.; Obata, K.; Kawabata, S.; Sugioka, K. λ/20 surface nanostructuring of ZnO by mask-less ultrafast laser processing. *Nanophotonics* **2023**, *12*, 1499–1510. [CrossRef]

26. Golubewa, L.; Rehman, H.; Padrez, Y.; Basharin, A.; Sumit, S.; Timoshchenko, I.; Karpicz, R.; Svirko, Y.; Kuzhir, P. Black Silicon: Breaking through the Everlasting Cost vs. Effectivity Trade-Off for SERS Substrates. *Materials* **2023**, *16*, 1948. [CrossRef]

27. Chen, H.; Shao, L.; Li, Q.; Wang, J. Gold Nanorods and Their Plasmonic Properties. *Chem. Soc. Rev.* **2013**, *42*, 2679–2724. [CrossRef]

28. Barbosa, S.; Agrawal, A.; Rodríguez-Lorenzo, L.; Pastoriza-Santos, I.; Alvarez-Puebla, R.A.; Kornowski, A.; Weller, H.; Liz-Marzán, L.M. Tuning Size and Sensing Properties in Colloidal Gold Nanostars. *Langmuir* **2010**, *26*, 14943–14950. [CrossRef]

29. Thien, N.D.; Dang, T.H.; Doanh, S.C.; Thao, L.Q.; Hoa, N.Q.; Dinh, N.N.; Hieu, N.M.; Vu, L.V. A study on fabrication of SERS substrates base on porous Si nanostructures and gold nanoparticles. *J. Mater. Sci. Mater. Electron.* **2023**, *34*, 94. [CrossRef]

30. Chirumamilla, A.; Moise, I.M.; Cai, Z.; Ding, F.; Jensen, K.B.; Wang, D.; Kristensen, P.K.; Jensen, L.R.; Fojan, P.; Popok, V.; et al. Lithography-free fabrication of scalable 3D nanopillars as ultrasensitive SERS substrates. *Appl. Mater. Today* **2023**, *31*, 101763. [CrossRef]

31. Xu, D.; Wang, Z.; Zhang, S.; Zhang, Y.; Yang, W.; Chen, J. Fabrication and SERS activity of high aspect ratio copper nanowires prepared via solid-state ionics method. *Phys. E Low-Dimens. Syst. Nanostruct.* **2023**, *153*, 115789. [CrossRef]

32. Hu, Y.; Cheng, H.; Zhao, X.; Wu, J.; Muhammad, F.; Lin, S.; He, J.; Zhou, L.; Zhang, C.; Deng, Y.; et al. Surface-enhanced raman scattering active gold nanoparticles with enzyme-mimicking activities for measuring glucose and lactate in living tissues. *ACS Nano* **2017**, *11*, 5558–5566. [CrossRef] [PubMed]

33. Athira, K.; Ranjana, M.; Bharathi, M.S.S.; Narasimha Reddy, B.; Satheesh Babu, T.G.; Venugopal Rao, S.; Ravi Kumar, D.V. Aggregation induced, formaldehyde tailored nanowire like networks of Cu and their SERS activity. *Chem. Phys. Lett.* **2020**, *748*, 137390. [CrossRef]

34. Zhang, C.; Chen, S.; Jiang, Z.; Shi, Z.; Wang, J.; Du, L. Highly Sensitive and Reproducible SERS Substrates Based on Ordered Micropyramid Array and Silver Nanoparticles. *ACS Appl. Mater. Interfaces* **2021**, *13*, 29222–29229. [CrossRef] [PubMed]

35. Khurana, K.; Jaggi, N. Localized Surface Plasmonic Properties of Au and Ag Nanoparticles for Sensors: A Review. *Plasmonics* **2021**, *16*, 981–999. [CrossRef]

36. Li, M.; Cushing, S.K.; Zhang, J.; Lankford, J.; Aguilar, Z.P.; Ma, D.; Wu, N. Shape-dependent surface-enhanced Raman scattering in gold-Raman-probe-silica sandwiched nanoparticles for biocompatible applications. *Nanotechnology* **2012**, *23*, 115501. [CrossRef] [PubMed]

37. Shan, B.; Pu, Y.; Chen, Y.; Liao, M.; Li, M. Novel SERS labels: Rational design, functional integration and biomedical applications. *Coord. Chem. Rev.* **2018**, *371*, 11–37. [CrossRef]

38. Yao, D.; Li, C.; Liang, A.; Jiang, Z. A facile SERS strategy for quantitative analysis of trace glucose coupling glucose oxidase and nanosilver catalytic oxidation of tetramethylbenzidine. *Spectrochim. Acta A Mol. Biomol. Spectrosc.* **2019**, *216*, 146–153. [CrossRef]

39. Weiss, S. Fluorescence spectroscopy of single biomolecules. *Science* **1999**, *283*, 1676. [CrossRef]

40. Kanioura, A.; Geka, G.; Kochylas, I.; Likodimos, V.; Gardelis, S.; Dimitriou, A.; Papanikolaou, N.; Kakabakos, S.; Petrou, P. SERS determination of oxidative stress markers in saliva using substrates with silver nanoparticle-decorated silicon nanowires. *Biosensors* **2023**, *13*, 273. [CrossRef]

41. Geka, G.; Kanioura, A.; Kochylas, I.; Likodimos, V.; Gardelis, S.; Dimitriou, A.; Papanikolaou, N.; Chatzantonaki, K.; Charvalos, E.; Economou, A.; et al. Cancer Marker Immunosensing through Surface-Enhanced Photoluminescence on Nanostructured Silver Substrates. *Nanomaterials* **2023**, *13*, 3099. [CrossRef] [PubMed]

42. Tsiasioti, A.; Georgiadou, E.; Zacharis, C.K.; Tzanavaras, P.D. Development and validation of a direct HPLC method for the determination of salivary glutathione disulphide using a core shell column and post column derivatization with o-phthalaldehyde. *J. Chromatogr. B Biomed. Appl.* **2022**, *1197*, 123216. [CrossRef] [PubMed]

43. Tarboush, N.A.; Al Masoodi, O.; Al Bdour, S.; Sawair, F.; Hassona, Y. Antioxidant capacity and biomarkers of oxidative stress in saliva of khat-chewing patients: A case-control study. *Oral Surg. Oral Med. Oral Pathol. Oral Radiol.* **2019**, *127*, 49–54. [CrossRef] [PubMed]
44. Miran, A.A.J.; Akram, H.M. Assessment of the salivary level of superoxide dismutase and melatonin in localized periodontitis versus generalized periodontitis. *Basrah J. Surg.* **2023**, *29*, 61–67. [CrossRef]
45. David, C.; d'Andrea, C.; Lancelot, E.; Bochterle, J.; Guillot, N.; Fazio, B.; Maragò, O.M.; Sutton, A.; Charnaux, N.; Neubrech, F.; et al. Raman and IR spectroscopy of manganese superoxide dismutase, a pathology biomarker. *Vib. Spectr.* **2012**, *62*, 50–58. [CrossRef]